



RESEARCH

Open Access

# A critical role for STIM1 in filopodial calcium entry and axon guidance

Sangwoo Shim<sup>1,2,3,4</sup>, James Q Zheng<sup>1,2\*</sup> and Guo-li Ming<sup>3,4,5</sup>

## Abstract

**Background:** Stromal interaction molecule 1 (STIM1), a  $\text{Ca}^{2+}$  sensor in the endoplasmic reticulum, regulates store-operated  $\text{Ca}^{2+}$  entry (SOCE) that is essential for  $\text{Ca}^{2+}$  homeostasis in many types of cells. However, if and how STIM1 and SOCE function in nerve growth cones during axon guidance remains to be elucidated.

**Results:** We report that STIM1 and transient receptor potential channel 1 (TRPC1)-dependent SOCE operates in *Xenopus* spinal growth cones to regulate  $\text{Ca}^{2+}$  signaling and guidance responses. We found that STIM1 works together with TRPC1 to mediate SOCE within growth cones and filopodia. In particular, STIM1/TRPC1-dependent SOCE was found to mediate oscillatory filopodial  $\text{Ca}^{2+}$  transients in the growth cone. Disruption of STIM1 function abolished filopodial  $\text{Ca}^{2+}$  transients and impaired  $\text{Ca}^{2+}$ -dependent attractive responses of *Xenopus* growth cones to netrin-1. Finally, interference with STIM1 function was found to disrupt midline axon guidance of commissural interneurons in the developing *Xenopus* spinal cord in vivo.

**Conclusions:** Our data demonstrate that STIM1/TRPC1-dependent SOCE plays an essential role in generating spatiotemporal  $\text{Ca}^{2+}$  signals that mediate guidance responses of nerve growth cones.

**Keywords:** Axon guidance, STIM1, SOCE, TRPC1, Calcium, Netrin-1, Filopodial  $\text{Ca}^{2+}$  entry,  $\text{Ca}^{2+}$  oscillation, Calcium homeostasis

## Background

Guided axonal growth and regeneration depend on the motile growth cone at the tip of axons to extend and navigate through a complex environment to reach specific targets for neuronal connections. It is well established that the nerve growth cone needs to maintain an optimal range of intracellular  $\text{Ca}^{2+}$  concentration ( $[\text{Ca}^{2+}]_i$ ) for its motility and responses to extracellular cues [1]. The cytoplasmic  $\text{Ca}^{2+}$  homeostasis is regulated by  $\text{Ca}^{2+}$  entry from the extracellular environment, internal  $\text{Ca}^{2+}$  release and replenishment of the intracellular store [2,3]. However, how neuronal growth cones coordinate guidance cue-induced  $\text{Ca}^{2+}$  influx, internal  $\text{Ca}^{2+}$  release and  $\text{Ca}^{2+}$  store replenishment to maintain proper guidance behaviors is unknown. Store-operated  $\text{Ca}^{2+}$  entry (SOCE) was originally characterized in non-excitabile cells as an indispensable

$\text{Ca}^{2+}$  influx mechanism to replenish internal stores [2,3]. It is triggered by  $\text{Ca}^{2+}$  depletion from ER through the ER  $\text{Ca}^{2+}$  sensor protein, stromal interacting molecule 1 (STIM1). In response to  $\text{Ca}^{2+}$  depletion, STIM1 oligomerizes and translocates to ER and plasma membrane junctions, where it interacts with and activates store-operated  $\text{Ca}^{2+}$  (SOC) channels that include TRPC1 and Orai1 proteins [2,3].

In the nervous system, SOCE has been seen to exist in a number of cell types [4-7] and implicated in synaptic plasticity, axon branching, neuropathic pain and fly motor circuit function [6-10]. However, the existence of SOCE and STIM1, and their potential contribution to the intracellular  $\text{Ca}^{2+}$  homeostasis and signaling in axon guidance is not well established. Axonal growth cones are highlighted by two types of actin-based motile membrane protrusions, filopodia and lamellipodia [11]. Of these two structures, lamellipodia are considered to be responsible for growth cone locomotion, whereas filopodia are believed to function in sensing of the environment during axon pathfinding [11-13]. Interestingly, rapid  $\text{Ca}^{2+}$  transients in growth cone filopodia have been shown to be

\* Correspondence: james.zheng@emory.edu

<sup>1</sup>Departments of Cell Biology and Neurology, Emory University School of Medicine, Atlanta, GA 30078, USA

<sup>2</sup>Center for Neurodegenerative Diseases, Emory University School of Medicine, Atlanta, GA 30322, USA

Full list of author information is available at the end of the article

involved in growth cone responses to extracellular cues [14,15]. But how  $Ca^{2+}$  signals are generated in filopodia and whether SOCE is involved in this process remain unknown. Here we report that SOCE operates in *Xenopus* spinal growth cones and depends on STIM1 and TRPC1. Importantly, we find that SOCE mediates spontaneous and netrin-1-potentiated filopodial  $Ca^{2+}$  entries within growth cones. We further provide evidence that STIM1- and TRPC1-dependent SOCE is required for attractive guidance responses of growth cones to netrin-1. Finally, we show that STIM1 is required for midline axon guidance of commissural interneurons in the developing *Xenopus* spinal cord *in vivo*. Our data suggest that SOCE is an essential component of intracellular  $Ca^{2+}$  homeostasis and signaling that regulate neuronal growth cone guidance.

## Results

### Cloning and expression of *Xenopus* STIM1

We first cloned *Xenopus* STIM1 (XSTIM1; 668 a.a.), which exhibited 72.8% identity to human STIM1 (685 a.a.; Additional file 1: Figure S1). Whole-mount *in situ* hybridization of developing *Xenopus* embryos showed that STIM1 is highly expressed in the dorsal part of the developing embryo, including the neural tube at stages when active axon guidance occurs (Figure 1A, top panels). Coronal sections of *Xenopus* embryos confirmed the expression of STIM1 mRNA in the neural tube, as well as in the notochord and somites (Figure 1A, bottom panels). RT-PCR analysis from dissected tissues further confirmed that XSTIM1 mRNA is expressed in neural tube and notochord of early tailbud *Xenopus* embryos (Figure 1B). Immunofluorescence analysis using anti-STIM1 antibody and fluorescent phalloidin to stain F-actin showed that STIM1 protein is ubiquitously distributed in *Xenopus* spinal neuron, including soma, neurites and growth cones (Figure 1C). Robust expression of XSTIM1 throughout the growth cone and in filopodia is better seen at higher magnifications (Figure 1D). These results show that *Xenopus* STIM1 is expressed in developing neural tissues and neuronal growth cones of developing axons.

### STIM1- and TRPC1-dependent SOCE in *Xenopus* neuronal growth cones

To study the function of STIM1 in growth cones, we generated wild-type (XSTIM1-WT) and two mutant forms of XSTIM1: a dominant negative form (DN, XSTIM1-D65A- $\Delta$ CT) and a constitutively active form (CA, XSTIM1-CT) (Figure 2A) based on previous studies of mammalian STIM1 mutants [16]. We first examined whether STIM1-dependent SOCE operates in neuronal growth cones by  $Ca^{2+}$  imaging analysis using fluo-4 calcium indicator. *Xenopus* neurons were first bathed in  $Ca^{2+}$ -free media with cyclopiazonic acid (CPA; 25  $\mu$ M), an endoplasmic reticulum  $Ca^{2+}$  pump inhibitor, to deplete intracellular

$Ca^{2+}$  stores. Subsequent addition of extracellular  $Ca^{2+}$  induced a marked and rapid rise in the intracellular  $Ca^{2+}$  concentration ( $[Ca^{2+}]_i$ ) in the growth cone (Figure 2B and C), suggesting the presence of functional SOCE in neuronal growth cones [4-7]. Importantly, we found that the SOCE was largely abolished in growth cones expressing either dominant negative *Xenopus* STIM1 (XSTIM1-DN, Figure 2B and 2C) or dominant negative human STIM1 (hSTIM1-DN) (Figure 2C), indicating that the elevation in  $[Ca^{2+}]_i$  requires the function of STIM1. In addition, knock-down of TRPC1 channels by morpholino oligonucleotides against XTRPC1 (XTRPC1-MO) abolished SOCE (Figure 2D). Therefore, TRPC1 is also an essential component of store-operated  $Ca^{2+}$  (SOC) channel complex as suggested by previous studies in saliva gland cells [17]. These results show that store-operated  $Ca^{2+}$  entry operates in neuronal growth cones and requires STIM1 and TRPC1.

### STIM1-dependent SOCE mediates netrin-1-induced $Ca^{2+}$ elevation in growth cones

Netrin-1 is known to guide axonal growth cone through a  $Ca^{2+}$ -dependent pathway [1,18] and netrin-1-induced increase in  $[Ca^{2+}]_i$  in growth cones requires both intracellular  $Ca^{2+}$  release and  $Ca^{2+}$  influx through channels on the plasma membrane [19-21]. Consistent with previous studies [21-23], bath application of netrin-1 (10 ng/ml final concentration) induced a significant rise in  $[Ca^{2+}]_i$  in *Xenopus* growth cones (Figure 2E). Importantly, overexpression of XSTIM1-DN abolished the sustained  $Ca^{2+}$  elevation within neuronal growth cones in response to netrin-1 (Figure 2E). Previous studies from ours and others have shown that TRPC1 is required for netrin-1-induced sustained  $Ca^{2+}$  elevation [21,23]. We have observed an association of TRPC1 with STIM1 in *Xenopus* brain lysates (Additional file 2: Figure S2), similar to what has been shown in mammalian cells [2,16,24]. Therefore, netrin-1 may activate STIM1-dependent SOCE through TRPC1 in neuronal growth cones.

### STIM1-dependent SOCE generates filopodial $Ca^{2+}$ entries in *Xenopus* neuronal growth cones

Localized  $Ca^{2+}$  transients in filopodia play an important role in filopodial motility and growth cone responses to extracellular cues [14]. We thus examined the potential role for SOCE in  $Ca^{2+}$  entry in growth cone filopodia. Here we used a membrane tethered calcium indicator Lck-GCaMP3 [25] to reliably monitor  $Ca^{2+}$  influx through the plasma membrane. Using a similar protocol as in Figure 2B-D, we measured both the incidence and frequency of fast  $Ca^{2+}$  entries in filopodia by high-speed (30 frames/sec) wide-field fluorescent imaging. We found that store  $Ca^{2+}$  depletion and re-addition of external  $Ca^{2+}$  experiment led to  $Ca^{2+}$  entries in about 25% filopodia

(Figure 3; Additional file 3: Movie 1). High frequency time-lapse traces of the integrated intensity of the Lck-GCaMP3 fluorescence and a kymograph representation clearly demonstrated that filopodial  $Ca^{2+}$  entries are independent of growth cone  $Ca^{2+}$  transients (Figure 3A-C; Additional file 3: Movie 1). Importantly, both the incidence and frequency of these filopodial  $Ca^{2+}$  entries were largely abolished by inhibition of XSTIM1 with XSTIM1-DN overexpression (Figure 3D and E; Additional file 4: Movie 2) or TRPC1 knockdown by XTRPC1-MO (Figure 3D and E; Additional file 5: Movie 3). These results thus indicate that STIM1- and TRPC1-dependent SOCE is indispensable for filopodial  $Ca^{2+}$  entries within neuronal growth cones.

Previous studies have revealed that *Xenopus* growth cones exhibit spontaneous filopodial  $Ca^{2+}$  transients that are closely associated with growth cone motility [14,15,26]. Using Lck-GCaMP3, we also observed robust periodic, spontaneous calcium entries in filopodia of *Xenopus* growth cones in a Modified Ringer solution that contains 1 mM extracellular  $Ca^{2+}$  (Figure 4A; Additional file 6: Movie 4). Importantly, both the incidence and frequency of the entries were also substantially reduced by inhibition of STIM1 and TRPC1 function (Figure 4B and C; Additional file 7: Movie 5 and Additional file 8: Movie 6), suggesting that STIM1/TRPC1-dependent SOCE is involved in generating and maintaining oscillatory patterns of spontaneous filopodial  $Ca^{2+}$  transients.

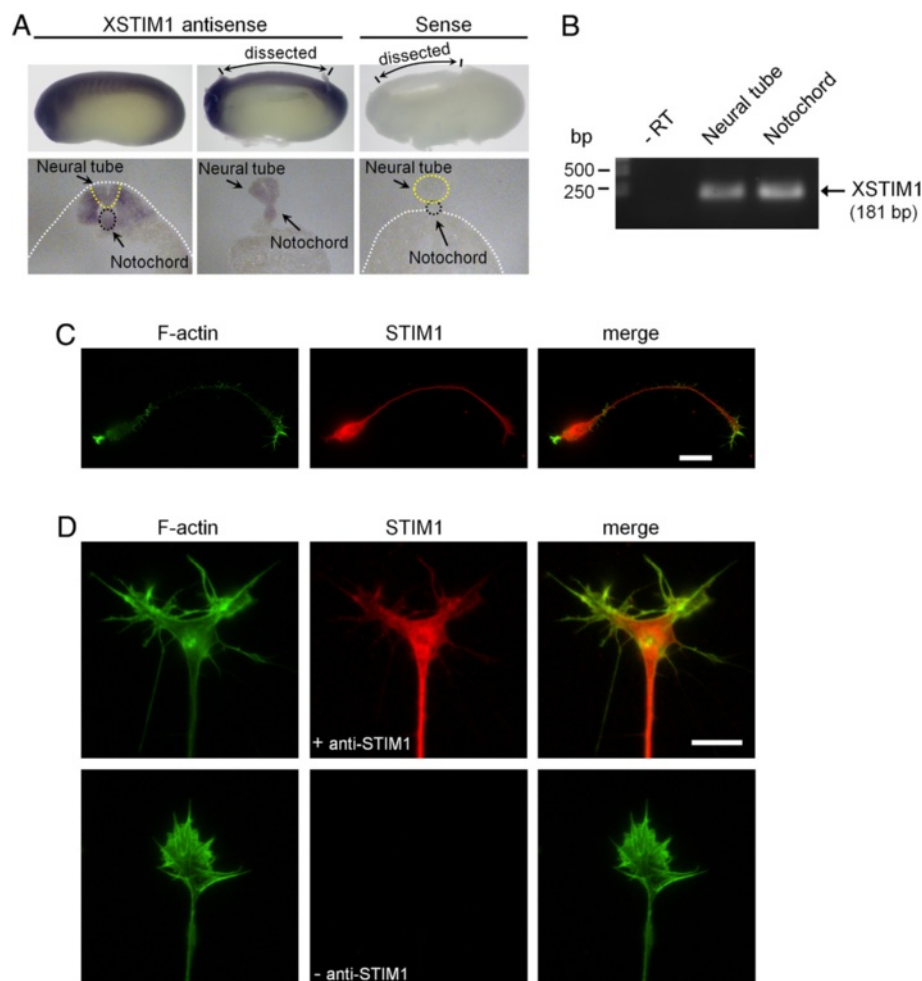


**Figure 1** *Xenopus* STIM1 is expressed in developing neural tissues and neuronal growth cones. (A) Sample images of whole-mount (top) and cross-section (bottom) *in situ* hybridization analysis of the mRNA expression of XSTIM1 in developing *Xenopus* embryos. Left, antisense; right, sense probe. Dotted lines delineate the boundaries of neural tube and notochord. (B) RT-PCR detection of XSTIM1 mRNA from RNA samples extracted from state 25-26 *Xenopus* neural tube and notochord tissues. -RT lane is the negative control of the RT-PCR on neural tube tissue RNA in the absence of a reverse transcriptase. (C) Representative immunofluorescence images of cultured *Xenopus* spinal neurons labeled for STIM1 (red) and F-actin (phalloidin: green). Scale bar: 20  $\mu$ m. (D) Representative immunofluorescence images of growth cones labeled for STIM1 (red) and F-actin (green). Negative control processed without STIM1 antibody (without STIM1, bottom) shows absence of immunolabeling. Scale bar: 10  $\mu$ m.

Bath application of netrin-1 (10 ng/ml final concentration) was found to potentiate both the incidence and frequency of filopodial  $\text{Ca}^{2+}$  entries of *Xenopus* spinal growth cones (Figure 4D-F; Additional file 9: Movie 7), consistent with previous study using Fluo-4 [15]. We found that this increase in filopodial  $\text{Ca}^{2+}$  entries by netrin-1 was abolished when STIM1 function was inhi-

bited by XSTIM1-DN (Figure 4E and F). Over-expression of morpholino against XTRPC1 (XTRPC1-MO) also compromised the potentiation of filopodial  $\text{Ca}^{2+}$  entries by netrin-1 (Figure 4E and F). Therefore, STIM1/TRPC1-dependent SOCE mediates the netrin-1-dependent potentiation of oscillatory filopodial  $\text{Ca}^{2+}$  entries in neuronal growth cones.

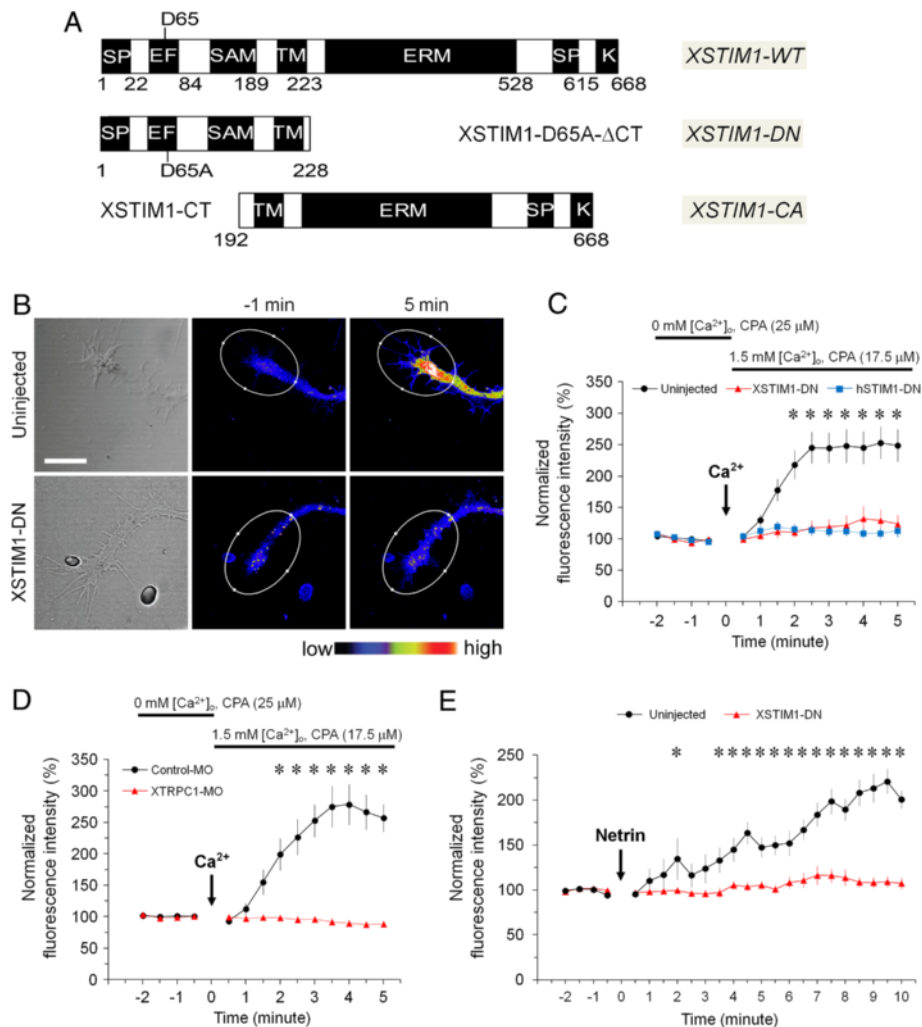


**Figure 2** STIM1-dependent SOCE operates and mediates netrin-1-induced  $\text{Ca}^{2+}$  elevation in *Xenopus* neuronal growth cones. **(A)** A schematic diagram of full-length wild-type (WT) and mutant constructs of XSTIM1. **(B)** Bright field and pseudocolor images of fluo-4 fluorescence of growth cones of *Xenopus* spinal neurons from the un.injected or mCherry-XSTIM1-DN injected embryos in the presence of CPA in  $\text{Ca}^{2+}$ -free media, before and after the re-addition of 1.5 mM  $\text{Ca}^{2+}$  bath solution. Pseudocolors indicate  $\text{Ca}^{2+}$  levels, with white as the highest and black as the lowest. Scale bar: 10  $\mu\text{m}$ . **(C)** Summary of internal  $\text{Ca}^{2+}$  store depletion-induced  $\text{Ca}^{2+}$  entry in growth cones at different time points before and after re-addition of 1.5 mM  $\text{Ca}^{2+}$ . The fluorescence intensity was normalized to the average fluorescence intensity of 2 min baseline levels prior to  $\text{Ca}^{2+}$  re-addition. Values represent mean  $\pm$  s.e.m. ( $n = 25$  for control,  $n = 10$  for XSTIM1-DN and  $n = 19$  for hSTIM1-DN; \* indicates  $P < 0.01$ ; Bootstrap-test). **(D)** XTRPC1 is required for store depletion-evoked  $\text{Ca}^{2+}$  entry in neuronal growth cones. Summary of internal  $\text{Ca}^{2+}$  store depletion-induced  $\text{Ca}^{2+}$  entry in growth cones from the control-MO or XTRPC1-MO injected embryos at different time points before and after the re-addition of 1.5 mM  $\text{Ca}^{2+}$ . Values represent mean  $\pm$  s.e.m. ( $n = 12$  for control, and  $n = 13$  for XTRPC1-MO; \* indicates  $P < 0.01$ ; Bootstrap-test). **(E)** XSTIM1 is required for netrin-1-induced  $\text{Ca}^{2+}$  elevation in growth cone. Summary of time course of  $\text{Ca}^{2+}$  changes in neuronal growth cones from un.injected or mCherry-XSTIM1-DN mRNA injected embryos. The fluorescence intensity was normalized to the average fluorescence intensity of 2 min baseline levels prior to the netrin-1 application (10 ng/ml). Values represent mean  $\pm$  s.e.m. ( $n = 6$  for control and  $n = 9$  for XSTIM1-DN; \* indicates  $P < 0.05$ ; Bootstrap-test).

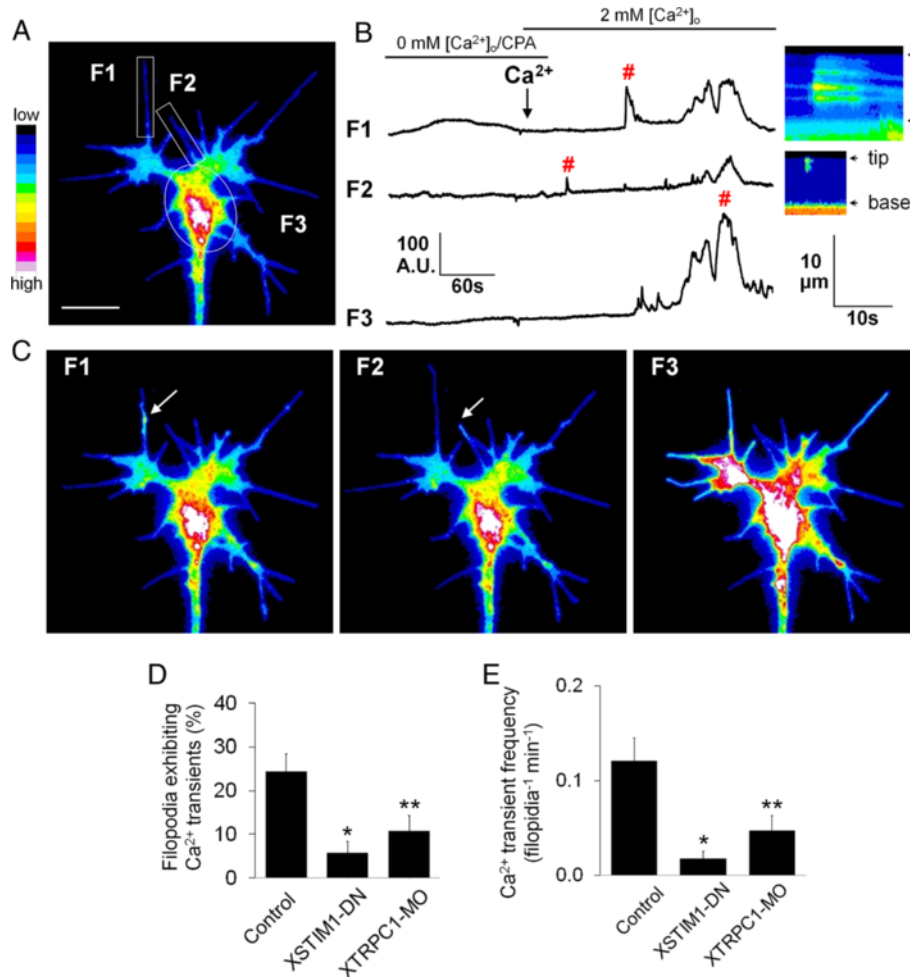


**Figure 3** STIM1-dependent SOCE generates filopodial Ca<sup>2+</sup> entries in *Xenopus* neuronal growth cones. **(A)** A pseudocolored Lck-GCaMP3 fluorescent Ca<sup>2+</sup> image of growth cone showing rectangular ROIs (region of interest) used to measure fluorescent intensities over time. Pseudocolors indicate Ca<sup>2+</sup> levels, with white as the highest and black as the lowest. Scale bar, 10  $\mu$ m. **(B)** Representative traces of Lck-GCaMP3 fluorescent Ca<sup>2+</sup> signals profile measured in two filopodia (F1, F2) and a growth center (F3) over 7 min period of store-depletion and re-addition of extracellular Ca<sup>2+</sup>. Images were captured at 200 milliseconds intervals. #, indicates filopodial and global Ca<sup>2+</sup> transients that are shown in **(C)**. Right images are kymographs generated from a segmented line along the filopodia from the tip to the base using NIH ImageJ. The arrowheads denote tip and base of filopodia. **(C)** Representative pseudocolored Lck-GCaMP3 fluorescent Ca<sup>2+</sup> images at the time point as indicated by # in **B**. The arrows show the initiation of filopodial Ca<sup>2+</sup> transients. **(D-E)** The incidence **(D)** and frequency **(E)** of filopodial Ca<sup>2+</sup> transients were determined in control (n = 21), XSTIM1-DN (n = 12), XTRPC1-MO (n = 10) expressing filopodia. \*P < 0.005 and \*\*p < 0.05 compared with control condition using t-test. Values represent mean  $\pm$  s.e.m.

The membrane tethered calcium indicator lck-GCaMP3 also provides an opportunity to map the entry sites of Ca<sup>2+</sup> in filopodia. We thus analyzed the sites of initial filopodial Ca<sup>2+</sup> entry in *Xenopus* growth cones by kymography analysis. We found that, although the initial sites of Ca<sup>2+</sup> entry distributed throughout the length of a filopodium, a large portion of the Ca<sup>2+</sup> entry sites (42-59%) were found at the filopodial tip (Figure 4G). When filopodial Ca<sup>2+</sup> entries under different conditions (store-operated, spontaneous, and netrin-1-induced) were examined, no difference was seen on the location of Ca<sup>2+</sup> entry sites in filopodia (Figure 4G). Therefore,

the tip of the filopodia appears to be the primary site of SOCE-mediated Ca<sup>2+</sup> entry in nerve growth cones.

STIM1 proteins reside predominantly in the ER, and undergo rapid and reversible translocation into ER-plasma membrane junctions to interact with and activate SOC channels following store depletion in non-excitable cells [27]. Live cell imaging of *Xenopus* neurons expressing YFP tagged STIM1 showed that YFP-XSTIM1-WT appeared to translocate into filopodia after store Ca<sup>2+</sup> depletion, as revealed by pseudocolored images and phase overlay images with mCherry (Figure 5; Additional file 10: Movie 8). Together with the presence of STIM1 in *Xenopus* growth



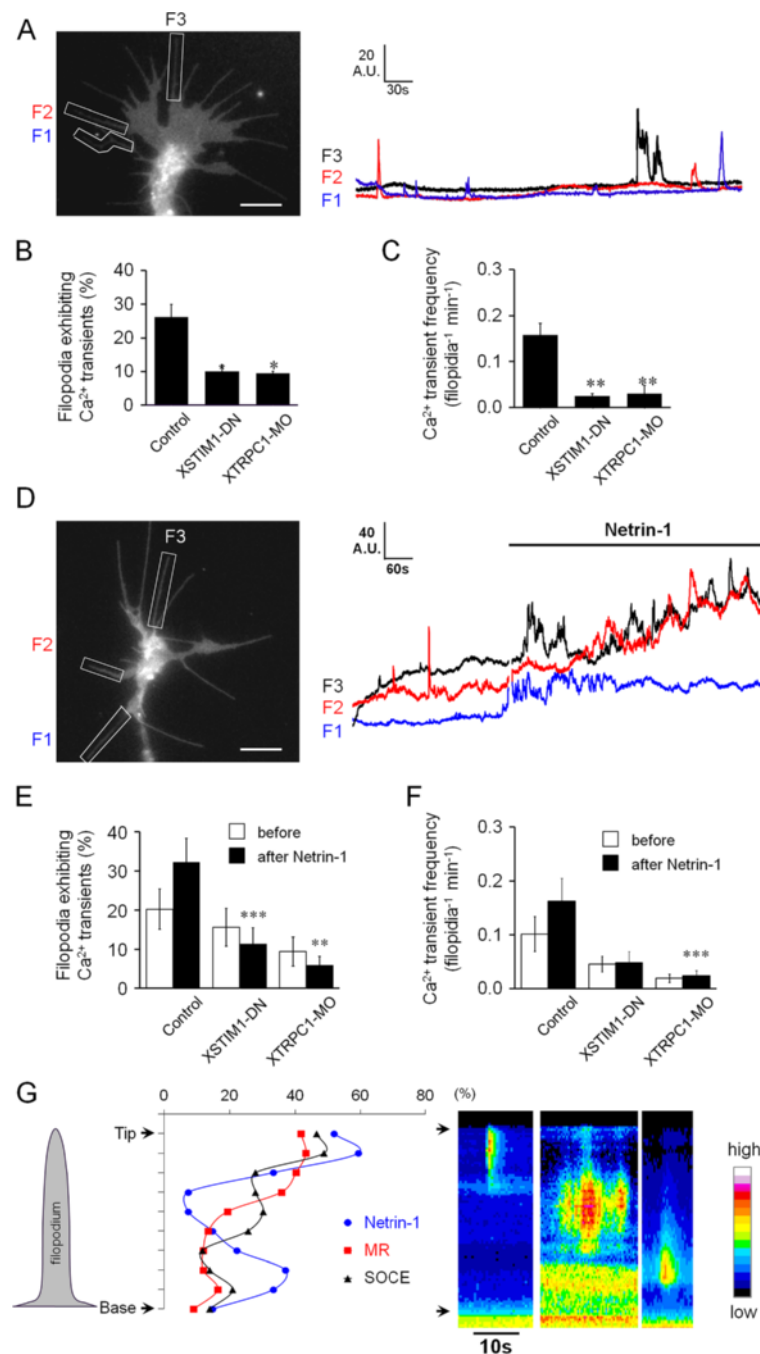


**Figure 4** STIM1/TRPC1-dependent SOCE mediates the spontaneous and netrin-1-potentiated filopodial Ca<sup>2+</sup> entries. **(A)** Left panel; a Lck-GCaMP3 fluorescent Ca<sup>2+</sup> image of a *Xenopus* spinal growth cone showing three ROIs (F1, F2 and F3) encompassing the filopodia used to measure fluorescent intensities over time (right panels). Scale bar, 10 μm. The incidence **(B)** and the frequency **(C)** of the spontaneous filopodial Ca<sup>2+</sup> transients were significantly attenuated by XSTIM1-DN (n = 30) or XTRPC1-MO (n = 30), when compared to the control (n=34; \*P < 0.001 and \*\*p < 0.005, Student's t-test). Values represent mean ± s.e.m. **(D)** A Lck-GCaMP3 fluorescent Ca<sup>2+</sup> image of a growth cone showing three ROIs (left panel) and their representative traces of Ca<sup>2+</sup> signals in three filopodia (F1, F2, F3) before and after bath application of netrin-1 (10 ng/ml) (right panel) in the presence of Sp-cAMP (25 μM). Scale bar, 10 μm. **(E-F)** Netrin-1 potentiated the incidence **(E)** and the frequency **(F)** of filopodial Ca<sup>2+</sup> transients in spinal growth cones (control; n = 14) and this potentiation was abolished by XSTIM1-DN (n = 8) and XTRPC1-MO (n = 10). \*\*\*P < 0.005 and \*\*\*\*p < 0.05 (Student's t-test). Values represent mean ± s.e.m. **(G)** Filopodia tips are the major site of initiation of filopodial Ca<sup>2+</sup> entry as revealed by kymographs of Ca<sup>2+</sup> signals in filopodia using Lck-GCaMP3 in modified Ringers saline (MR; n = 67), netrin-1 exposure (n = 27) and Ca<sup>2+</sup> re-addition after depletion (SOCE; n = 43). The y axis represents the path distance along the filopodia divided into 10 portions and the x axis represents time. The arrows denote the tip and base of filopodia.

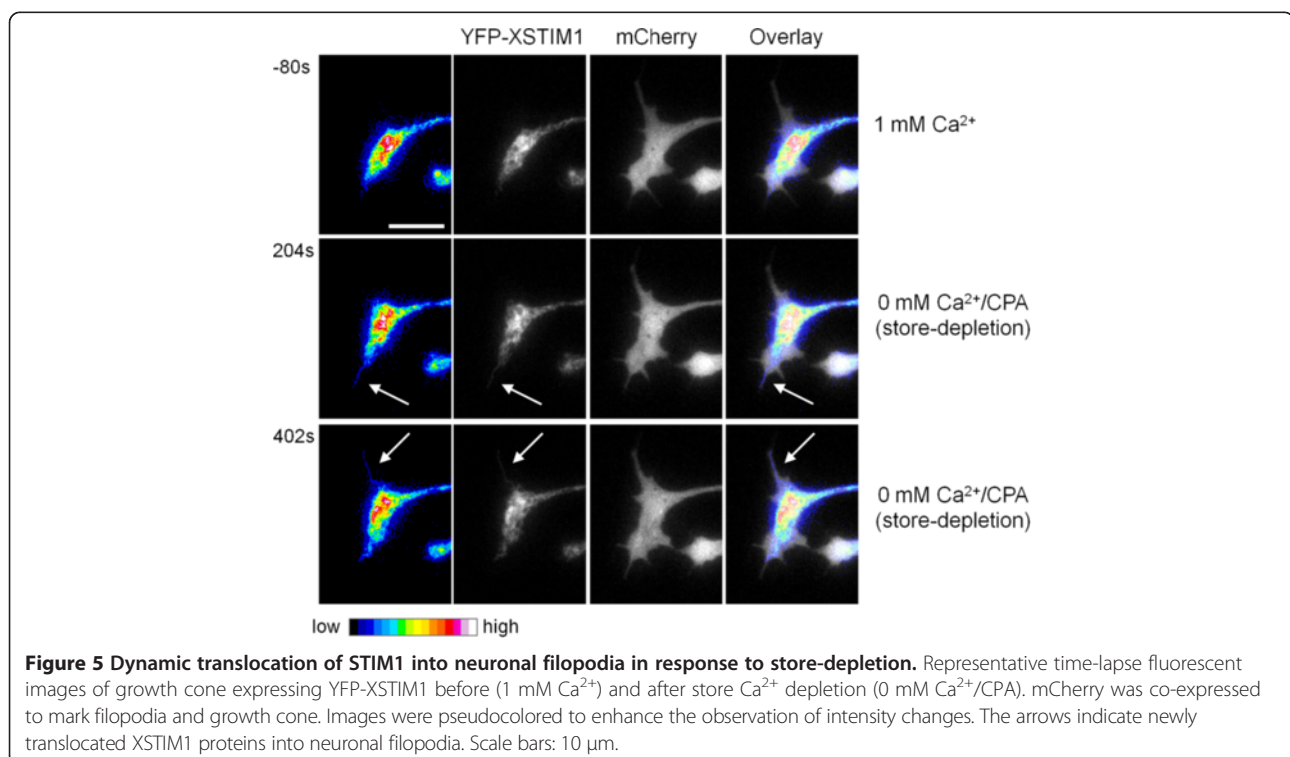
cones and their filopodia by immunostaining (Figure 1D), these results suggest an intriguing possibility that STIM1 proteins may become spatially reorganized into growth cone filopodia after activation by store-depletion to further activate SOC channels that may include TRPC1.

#### XSTIM1 is required for growth cone guidance

To test whether STIM1-dependent SOCE is required for growth cone guidance in response to netrin-1, we employed a well-established *in vitro* growth cone turning assay [19,20,23,28]. Previous studies have shown that netrin-1, a classical guidance cue, induces growth cone turning responses that are mediated by  $Ca^{2+}$  from both extracellular and intracellular sources [19-21,29]. In a microscopic gradient of netrin-1 (5  $\mu$ g/ml in the pipette, ~5 ng/ml reaching the growth cone), *Xenopus* growth cones of overnight culture (12-20 hrs) without laminin coating exhibited robust chemoattractive turning within 30 minutes (Figure 6A). Importantly, expression of XSTIM1-DN or XSTIM1-CA in *Xenopus* spinal neurons completely abolished netrin-1-induced attraction, and interestingly resulted in repulsion (Figure 6A and B). Expression of wild-type STIM1 (WT) produced no effect on netrin-1-induced attractive turning (Figure 6A and B). Over-expression of the dominant negative human STIM1 (hSTIM1-DN) [16] also eliminated netrin-1-induced attraction and converted it to repulsion (Figure 6B). The neurite extension rate in a netrin-1 gradient was not

significantly different under these conditions [29], except XSTIM1-CA which slightly reduced the growth rate (Figure 6C). Thus, proper function of XSTIM1 is essential for netrin-1-induced growth cone turning responses of *Xenopus* spinal neurons *in vitro*. Together with the previous studies showing that TRPC1 knock-down abolished the netrin-1-induced attractive growth cone turning responses [20,21], the results indicate that STIM1/TRPC1-dependent SOCE may play a critical role in growth cone guidance.

To assess whether STIM1 is required for axon guidance *in vivo*, we examined the midline axon guidance of commissural interneurons in the developing *Xenopus* spinal cord, which is known to require netrin-1 signaling [20,23]. Commissural interneuron axons in developing *Xenopus* embryos were specifically identified with the 3A10 monoclonal antibody [20]. In stage 25-26 embryos, 3A10-positive commissural axons extend toward and across the midline in a highly organized manner (Figure 7A and B). In contrast, a significant percentage of commissural axons derived from YFP-XSTIM1-DN injected embryos wandered around and failed to cross the midline with some even went out of the spinal cord (Figure 7C). For simplicity, we scored both types of guidance defects as the one not crossing and presented and quantified the percentage of crossed axons (Figure 7F). XSTIM1-DN markedly reduced the percentage of crossed axons to about 50% of the control groups (uninjected and GFP injection only)



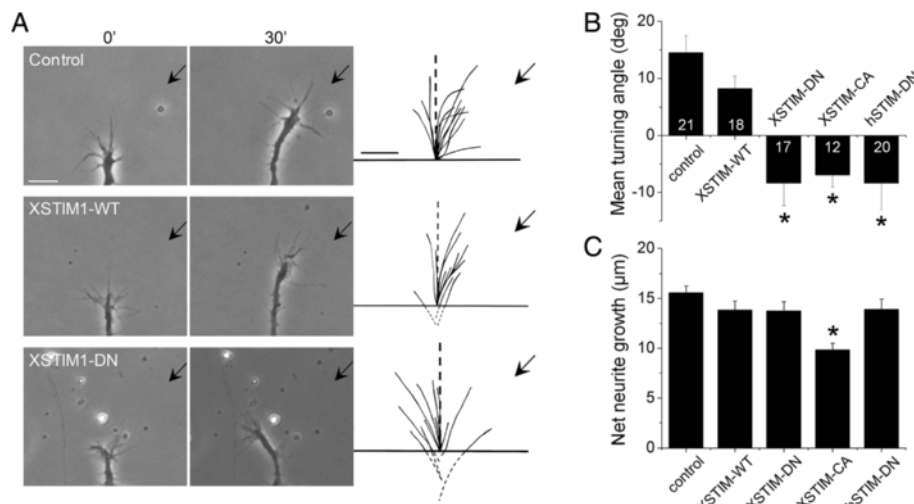


**Figure 6** XSTIM1 is required for attractive turning responses of neuronal growth cones to a netrin-1 gradient. **(A)** Sample images of growth cone turning responses in a gradient of netrin-1 of a control *Xenopus* spinal neuron, and neurons derived from embryos injected with mRNA encoding wild-type (YFP-XSTIM1-WT), or dominant negative mutant (YFP-XSTIM1-DN). The left two columns of images show neuronal growth cones at the start (0 min) and the end of exposure (30 min) to a netrin-1 gradient (5 µg/ml in the pipette). The right column shows superimposed trajectories of neurite extension during the 30' period for a sample population of 12 neurons under the each condition. The origin is the center of the growth cone and the original direction of growth is vertical. Arrows indicate the direction of the gradient. Scale bars: 10 µm. **(B)** Summary of mean turning angles of growth cones in responses to a gradient of netrin-1 under different conditions. The number associated with the bar graph indicates the number of growth cones analyzed. Values represent mean ± s.e.m. (\* indicates  $P < 0.01$ ; Bootstrap-test). **(C)** Summary of net neurite growth during the 30 minutes turning assay under different conditions. Values represent mean ± s.e.m. (\* indicates  $P < 0.05$ ; Bootstrap-test).

and the WT group. Similarly, over-expression of YFP-XSTIM1-CA, but not YFP-XSTIM1-WT, also led to significant midline guidance defects (Figure 7D and F). On the other hand, none of these molecular manipulations significantly affected the numbers of commissural neurons in the developing *Xenopus* spinal cord (Figure 7G). Taken together, these results demonstrated that STIM1 is required for the midline axon guidance of commissural interneurons in the developing *Xenopus* spinal cord in vivo.

## Discussion

$Ca^{2+}$  is a key second messenger that mediates a wide range of neuronal activity and responses to extracellular stimuli [1]. Spatiotemporally-restricted  $Ca^{2+}$  signals can steer growth cones in responses to extracellular guidance cues and are thought to be generated from  $Ca^{2+}$  influx through the plasma membrane as well as  $Ca^{2+}$  release from internal store [1,18]. However, how these two events are coupled to sustain  $Ca^{2+}$  signaling during guidance responses remain unclear. SOCE is believed to be a part of the intracellular  $Ca^{2+}$  homeostasis machinery that maintains  $[Ca^{2+}]_i$  for various neuronal functions, including optimal growth cone motility. The function of SOCE is well established in non-excitable cells and considered as a  $Ca^{2+}$  entry mechanism for refilling intracellular  $Ca^{2+}$  stores. The molecular components of SOCE include STIM, Orai, and TRP channels, which have also been

identified and characterized mostly in non-excitable cells [2,3]. More recently, several studies support the presence and functional implication of SOCE in the nervous system [4-9], but the molecular composition and functional role of SOCE and STIM1 in neuronal growth cone guidance is not well established. Our data demonstrate that STIM1- and TRPC1-dependent SOCE not only operates in neuronal growth cones but also mediates filopodial  $Ca^{2+}$  transients and growth cone guidance both in vitro and vivo [20,30,31]. Our results are consistent with a recent report showing that STIM1 and Orai, two components of SOCE, are involved in growth cone responses to brain derived neurotrophic factor and Semaphorin-3a [32]. Importantly, our study has further identified that TRPC1 is also an essential component of SOCE and a major site of SOCE-mediated  $Ca^{2+}$  entry is in the filopodia, especially at the tip of the filopodia. Moreover, we have presented in vivo evidence that STIM1 is required for proper guidance of commissural axons in developing spinal cord, a classic example of netrin-1-dependent long-range growth cone guidance [20,30,31]. Together, the current study has clearly established a role for SOCE, involving STIM1 and TRPC1, in mediating filopodial  $Ca^{2+}$  entries underlying axonal growth cone guidance.

At this moment, the precise mechanism by which STIM1 and SOCE are involved in netrin-1-induced  $Ca^{2+}$



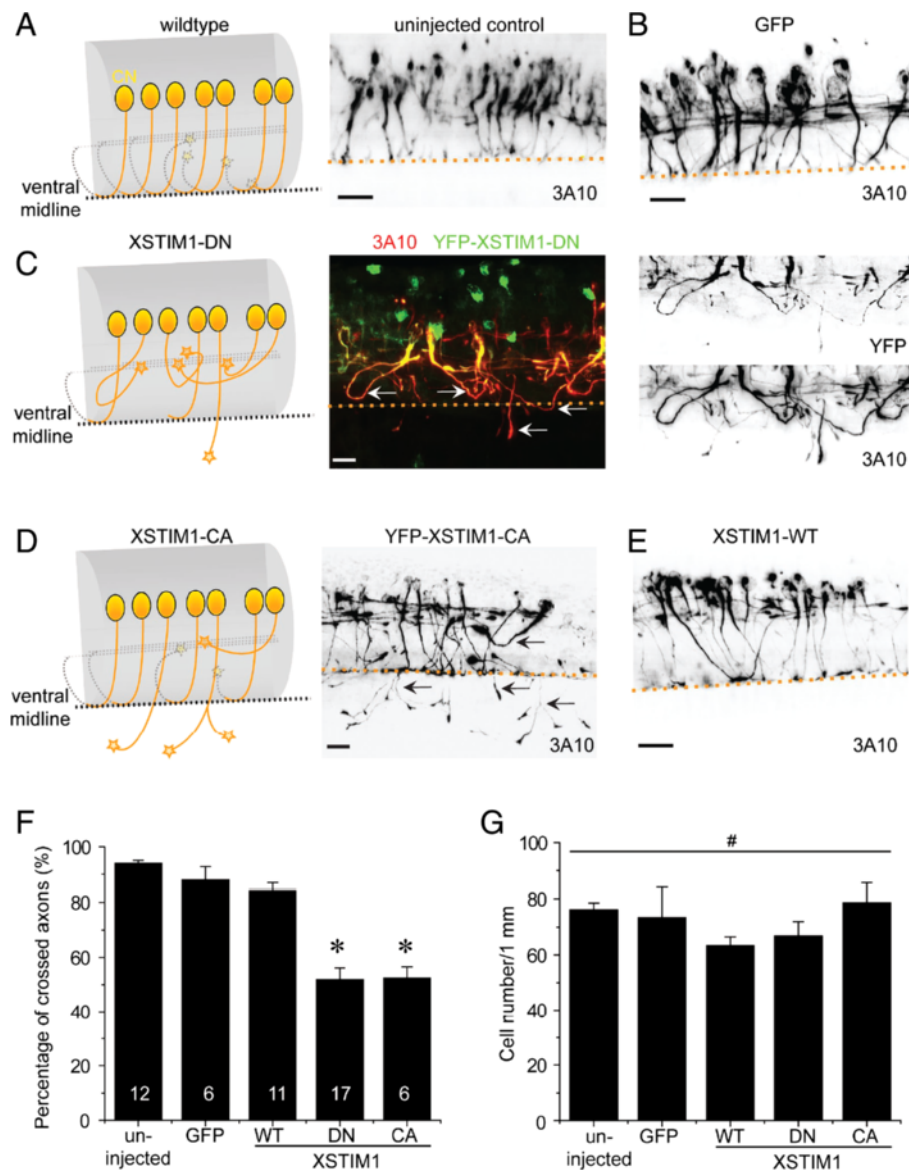


**Figure 7** XSTIM1 is required for midline axon guidance of commissural interneurons in the developing *Xenopus* spinal cord. (A-E)

Sample images of the sagittal view of commissural interneurons and their axonal projections in the *Xenopus* spinal cord from stage 25-26 embryos. Shown are schematic diagrams and confocal z-stack projection images of 3A10 staining of commissural interneuron axons from uninjected embryos, or embryos injected with mRNAs for GFP (B), YFP-XSTIM1-DN (C), YFP-XSTIM1-CA (D), or YFP-XSTIM1-WT (E), at the two to four cell-stage to manipulate a sub-population of neurons. Dotted line represents ventral midline; arrows point to mis-targeted axons. Scale bars: 20  $\mu$ m. (F) Quantification of the percentage of 3A10<sup>+</sup> commissural interneurons with normal midline crossing under different experimental conditions. The number associated with the bar graph indicates the number of embryos examined under each condition. Values represent mean  $\pm$  s.e.m. (\* indicates  $P < 0.01$ ; Bootstrap-test). (G) Summary of the density of 3A10<sup>+</sup> commissural neurons under each condition. The same embryos as in (F) were examined. Values represent mean  $\pm$  s.e.m. (# indicates  $P > 0.1$ ; Bootstrap-test).

signaling for growth cone attraction remains unclear. Netrin-1 is known to elicit Ca<sup>2+</sup> signals by Ca<sup>2+</sup> influx through TRPC1 and Ca<sup>2+</sup> release from the internal stores to induce growth cone attraction [1,18-20] but the underlying mechanism remains unclear. It has been shown that brain derived neurotrophic factor (BDNF) triggers Ca<sup>2+</sup> release from internal stores through activation of the PLC- $\gamma$  and IP<sub>3</sub> pathway, which in turn induces SOCE

through STIM1-TRPC activation [18,32-34]. Netrin-1 is considered to be in the same group of Ca<sup>2+</sup>-mediated guidance cues with BDNF. Given that PLC- $\gamma$  and IP<sub>3</sub>-induced Ca<sup>2+</sup> release are involved in growth cone extension and navigation [22,34-36], we propose that netrin-1 may initiate intracellular Ca<sup>2+</sup> release through activation of netrin-1 receptor Deleted in Colorectal Cancer (DCC), PLC- $\gamma$  and IP<sub>3</sub> production, which further triggers store-

depletion, STIM1 activation, and  $\text{Ca}^{2+}$  influx through TRPC1 for replenishing ER  $\text{Ca}^{2+}$ . This notion is further supported by the findings that both netrin-1 and BDNF activate PLC- $\gamma$  and Phosphatidylinositol 4,5-bisphosphate (PIP<sub>2</sub>) hydrolysis in neurite elongation [37,38]. Therefore, our results provide additional evidence for the conserved signaling pathways among  $\text{Ca}^{2+}$ -mediated guidance cues and between netrin-1 and neurotrophins.

The role of TRPC channels as SOCs has been controversial, but multiple lines of evidence support TRPC as a strong candidate component of store-operated  $\text{Ca}^{2+}$  channels. For example, TRPC1 has been shown to be bound and activated by STIM1 and contribute to SOCE in some cells [16,17,39-41]. We found that STIM1 interacts with TRPC1 in embryonic neural tissues (Additional file 2: Figure S2) and that TRPC1 knockdown inhibits STIM1-mediated SOCE within growth cones and filopodia (Figures 2D, 3D and 3E), suggesting that TRPC1 is an essential component of SOCE. As STIM1 is also required for netrin-1-induced  $\text{Ca}^{2+}$  elevation and growth cone attraction which was shown to be mediated by TRPC1, our data support a role for STIM1 in activating TRPC1. However, we cannot rule out the possibility that STIM1 may affect  $\text{Ca}^{2+}$  signaling and growth cone guidance by other mechanisms, such as its effects on cAMP signaling or ER remodeling [42,43]. Recent studies also showed biochemical assembly of STIM1-TRPCs-Orai complex and functional connections between TRPC channels and Orai1 [41,44,45]. STIM1-Orai1 co-localization in response to  $\text{Ca}^{2+}$  depletion was reported in neuronal growth cones [32]. Therefore, it is possible that Orai also plays a role in netrin-1 signaling and guidance.

It should be noted that Lck-GCaMP3 was successfully used in distinguishing the  $\text{Ca}^{2+}$  signals from membrane entry from internal release from the stores [25,46]. Our data with Lck-GCaMP3 showing the presence of filopodial  $\text{Ca}^{2+}$  transients and its potentiation by netrin-1 is consistent with the previous reports using Fluo-4 [14,15,26]. However, when compared with previous studies using Fluo-4, the incidence and frequency of filopodial  $\text{Ca}^{2+}$  transients observed in our study appear to be lower than those seen in the previous reports. The difference may be attributed to two possibilities. First, Lck-GCaMP3 detects  $\text{Ca}^{2+}$  entry events only at near-plasma membrane regions. However, Fluo-4 could detect cytosol  $\text{Ca}^{2+}$  changes from other sources such as intracellular stores, which will likely be missed by Lck-GCaMP3. In this regard, Lck-GCaMP3 fluorescence  $\text{Ca}^{2+}$  signals may be better called "filopodial  $\text{Ca}^{2+}$  entries" rather than filopodial  $\text{Ca}^{2+}$  transients. Second, we did not count the  $\text{Ca}^{2+}$  transients propagated from the growth cone proper and only counted the  $\text{Ca}^{2+}$  entry events generated within the filopodium independently of  $\text{Ca}^{2+}$  transients from the growth cone proper. Therefore, our data do not contradict the previous work.

It is of interest to see that the initial site of filopodial  $\text{Ca}^{2+}$  entry is largely localized to the tip of filopodia. Filopodia are considered to be the sensory apparatus for growth cones as they extend farther distance to detect the environmental signals. Therefore, it makes sense to have the sensory molecules accumulated at the tip for signal transduction initiation. However, the lack of quality antibodies prevented us from convincingly detecting the localization of STIM1/TRPC1 and other SOCE components at the filopodial tip. On the other hand, it has been reported that several receptors such as integrins, TRPC1 and DCC [14,26,47] and signaling molecules such as Src, PAK, PKA [48,49] are enriched at the tip of filopodia along with many other cytoskeleton regulatory molecules [11,50,51]. Therefore, it is conceivable that STIM1 and TRPC1 could function at the filopodial tip as an effective way to sense the environment and initiate  $\text{Ca}^{2+}$  signaling during growth cone guidance.

We report fast, highly localized and periodic spontaneous filopodial  $\text{Ca}^{2+}$  entries initiated independently of growth cone  $\text{Ca}^{2+}$  transients, which was consistent with the previous reports of oscillatory pattern of spontaneous  $\text{Ca}^{2+}$  transients within growth cone and filopodia during axonal growth [14,15,52]. The critical role for TRPC1 in generation of filopodial  $\text{Ca}^{2+}$  entry and its potentiation by netrin-1 is also consistent with the previous reports [14,15,26]. A further unexpected result was that STIM1-DN mutant blocked not only the SOCE-induced filopodial  $\text{Ca}^{2+}$  entries that depend on STIM1 but also spontaneous and netrin-1-potentiated oscillatory filopodial  $\text{Ca}^{2+}$  entries, suggesting that STIM1-dependent SOCE mediates the generation and maintenance of filopodial  $\text{Ca}^{2+}$  entries. Thus, our visualization of oscillatory patterns of spontaneous filopodial  $\text{Ca}^{2+}$  entries and their inhibition by STIM1- or TRPC1-knockdown is the first demonstration of a role of STIM/TRPC1-dependent SOCE in regulating  $\text{Ca}^{2+}$  oscillation in neurons, which is consistent with previous findings in other cell types [53-55]. It is plausible that store  $\text{Ca}^{2+}$  release, transient drop in ER  $\text{Ca}^{2+}$ , and  $\text{Ca}^{2+}$  entry through TRPC1 triggered by transient STIM1 activation may underlie the  $\text{Ca}^{2+}$  oscillations seen in growth cone filopodia. Thus, considering the functional correlation between the frequency of filopodial  $\text{Ca}^{2+}$  transients and growth cone outgrowth and turning [14,26], disruption of STIM1 or TRPC1 function is likely to result in the breakup of  $\text{Ca}^{2+}$  cycling for oscillations and subsequent attenuated frequency of filopodial  $\text{Ca}^{2+}$  entries, which may further cause the suppression of growth cone guidance in response to netrin-1.

## Conclusions

Our data demonstrate a role for STIM1/TRPC1-dependent SOCE in mediating oscillatory patterns of spontaneous and

netrin-1-potentiated filopodial  $\text{Ca}^{2+}$  entries that underlie axonal growth cone guidance both in vitro and in vivo.

## Methods

### Molecular constructs

*Xenopus* STIM1 (XSTIM1) [GenBank: BC126011] was identified by BLAST searches of the GenBank database using human STIM1 cDNA sequence. The coding region of XSTIM1 gene was isolated by RT-PCR, sequenced and cloned into the pCS2 vector (gift of D. Turner, University of Michigan). The following constructs of XSTIM1 and its mutants were generated by site-directed mutagenesis (Stratagene) or by PCR based on previous studies of mammalian STIM1 mutants [16]: YFP-XSTIM1-WT, YFP-XSTIM1-DN, YFP-XSTIM1-CA, and mCherry-XSTIM1-DN (Figure 2A). Different XSTIM constructs were *in vitro* transcribed with the mMESSAGE mMACHINE SP6 kit (Ambion). pN1-Lck-GCaMP3 plasmid was obtained from Addgene (plasmid #26974, [25]), cloned into pCS2 vector using BamHI and XbaI sites and *in vitro* transcribed with mMESSAGE mMACHINE SP6 kit (Ambion).

### Xenopus embryo injection and spinal neuron culture

Blastomere injections of mRNAs or morpholinos into early stages of *Xenopus* embryos and culturing of spinal neurons from these injected embryos were performed as previously described [20,23,29,56]. Briefly, fertilized embryos were injected at the two- or four-cell stage with mRNA (2-3 ng/embryo). A control morpholinos or morpholinos specific for *Xenopus* TRPC1 (XTRPC1-MO) was previously described [20]. Uninjected or injected embryos at stage 22 were used for cultures of spinal neurons as previously described [20,23]. All the procedures involving *Xenopus* frogs and embryos were carried out in accordance to the NIH guideline for animal use and have been approved by the Institutional Animal Care and Use Committee (IACUC) of Emory University.

### RT-PCR and Whole-mount *in situ* hybridization of *Xenopus* embryos

Neural tube and notochord were isolated from the dorsal section of the stage 25-26 *Xenopus* embryos after dissection with microsurgical scissors and incubation with collagenase (type I, Sigma). Total RNA was prepared by using TRIzol Reagent (Invitrogen) and treated with the RNase-free DNase I (Roche) to remove genomic DNA. The extracted RNA was reverse transcribed by using M-MLV reverse transcriptase (Invitrogen) and random hexamers (Roche). PCR amplification was performed using Taq polymerase (Fermentas). The -RT lane is the negative control of the RT-PCR on neural tube tissue RNA in the absence of a reverse transcriptase. The PCR primers are as follows; XSTIM1-forward, 5' CCAGAACCTTGAA

GAGGTG 3', XSTIM1-reverse, 5' GACTGAATGGTAC CGGCTGT 3'; XODC-forward, 5' CAGCTAGCTGTG GTGTGG 3', XODC-rev, 5' CAACATGGAACTCA-CACC 3'. For whole-mount *in situ* hybridization, the digoxigenin (DIG)-UTP-labelled antisense RNA was used as previously described [23,57]. The C-terminal region of XSTIM1 corresponding to amino acid 192-668 was used for the specific anti-sense and sense probes. The labelled probe was detected with alkaline phosphatase-conjugated anti-DIG antibody (Fab fragments) and visualized with the BM purple AP substrate (Roche Applied Science). Selected embryos from whole-mount *in situ* hybridization were embedded in a sucrose and Tissue-Tek O.C.T medium, completely frozen and cross-sectioned at 40  $\mu\text{m}$  with a cryostat (Leica CM1850).

### Immunocytochemistry

*Xenopus* spinal neuron cultures were fixed in 4% paraformaldehyde in a cacodylate buffer (0.1 M sodium cacodylate, 0.1 M sucrose, pH 7.4) for 30 minutes and permeabilized with Triton X-100 (0.1%) for 10 minutes. The cells were incubated with a rabbit polyclonal antibody against full length human STIM1 (MyBioSource) at a dilution of 1:50 after blocking with 5% goat serum and labelled with Alexa Fluor 546 goat anti-rabbit secondary (Invitrogen). Fluorescent imaging was captured on an inverted microscope (Nikon Eclipse Ti-E).

### Growth cone turning assay

Microscopic gradients of netrin-1 (5  $\mu\text{g}/\text{ml}$  in the pipette) were produced as previously described [29,56,58,59]. *Xenopus* spinal neurons derived from injected blastomeres were identified under fluorescent microscope and used for turning assay at the room temperature 14 to 20 hrs after plating as previously described [20,23,29,56]. The culture was plated on glass coverslip without any coating. The turning angle was defined by the angle between the original direction of neurite extension and a straight line connecting the positions of the center of the growth cone at the onset and the end of the 30 min period. The rates of neurite extension were calculated based on the net neurite extension during the turning assay. Only those growth cones of isolated neurons with a net neurite extension > 5  $\mu\text{m}$  over the 30-min period were included for analysis. Statistical significance was assessed using the Bootstrap-test.

### $\text{Ca}^{2+}$ imaging of cultured *Xenopus* spinal neurons

$\text{Ca}^{2+}$  imaging of cultured growth cones of *Xenopus* spinal neurons was performed as previously described [23,29,56]. Specifically, isolated *Xenopus* spinal neurons were cultured on glass coverslip without coating, loaded with Fluo-4 AM (2  $\mu\text{M}$ , Molecular Probes) for 30 minutes, rinsed with the Modified Ringer used for growth cone



turning assay, and imaged after bath-application of netrin-1 (10 ng/ml). For store-operated  $\text{Ca}^{2+}$  entry experiment, neurons were bathed in  $\text{Ca}^{2+}$ -free media with CPA (25  $\mu\text{M}$ ) to deplete intracellular  $\text{Ca}^{2+}$  stores, and imaged after re-addition of extracellular  $\text{Ca}^{2+}$  (1.5 mM). Growth cones expressing mCherry-XSTIM1-DN proteins were identified under fluorescent microscope and selected for further  $\text{Ca}^{2+}$  imaging. Imaging was carried out using a Zeiss 510 META system equipped with a 20X objective (NA 0.8). Excitation was at 488 nm by argon laser and the emitted fluorescence was collected at 500-560 nm. Fluorescence and bright-field images were simultaneously acquired at every 30 seconds with a frame scan. The mean fluorescence intensity of each time point was measured over a fixed circular region of interest that covers the entire growth cone and normalized to the average fluorescence intensity that was measured during a 2 minutes baseline period (prior to the netrin-1 application or addition of 1.5 mM  $\text{Ca}^{2+}$  solution).

For filopodial  $\text{Ca}^{2+}$  imaging, Lck-GCaMP3 mRNA was injected into early staged embryos without or with other mRNAs or morpholino. Spinal neurons were cultured on the glass coverslip coated with poly-D-lysine and laminin, which increases the number and length of filopodia [60], in serum-free culture medium. In our netrin-1-induced filopodial  $\text{Ca}^{2+}$  entries experiments, the spinal neurons were incubated in MR solution with the addition of cAMP analog Sp-cAMP (25  $\mu\text{M}$ ) to counterbalance the laminin's effect of reducing cAMP levels in growth cones [61] and mimic the condition of our *in vitro* turning assay where laminin coating on the glass culture dish was omitted. Live cell imaging of  $\text{Ca}^{2+}$  transients was performed on an inverted microscope (Nikon Eclipse Ti-E) equipped with a 60X Apo TIRF objective (NA 1.49), and EMCCD camera (Photometrics) using NIS-Elements software (Nikon). Excitation was at 488 nm and the emitted fluorescence was collected at 520 nm and Lck-GCaMP3 fluorescence images were acquired at every 200 milliseconds. To determine several characteristics of filopodial  $\text{Ca}^{2+}$  entries, including the incidence, frequency and initiation sites of transients, the Kymographs (spatio-temporal map) were created from the images of the user-defined segmented line one pixel in width spanning the filopodium from the time-lapse movies with NIH ImageJ software. Grayscale values for this linear region of interest (ROI) for each frame of the time series were transformed into pseudocolored images to show time-dependent changes in intracellular  $\text{Ca}^{2+}$  concentration ( $[\text{Ca}^{2+}]_i$ ) along the length of the ROI (y-axis) over time (x-axis).

#### Immunoprecipitation and immunoblotting

For co-immunoprecipitation, protein lysates were prepared from the *Xenopus* brain explants including spinal cords dissected from the embryos at stage 26-28 using

lysis buffer containing 1% Triton X-100, 150 mM NaCl, 10 mM Tris-Cl (pH 7.4), 1 mM EDTA, 1 mM EGTA, 0.5% Nonidet P-40, 0.2 mM Na-orthovanadate, and protease inhibitor cocktail. They were incubated with the appropriate antibody for 3-4 hours at 4°C, followed by incubation with protein A/G agarose beads (Pierce) for overnight at 4°C. Mouse anti-c-Myc monoclonal antibody (Roche Applied Science) and rabbit anti-GFP polyclonal antibody (Abcam) were used for immunoprecipitation and immunoblotting.

#### Whole-mount immunocytochemistry

Embryos at stage 25-26 were fixed and processed for immunocytochemistry as previously described [20,23,62]. Monoclonal antibody 3A10, specific for commissural interneurons [23,63], was obtained from the Developmental Studies Hybridoma Bank at the University of Iowa and used at a dilution of 1:100. Secondary antibodies were used at a dilution of 1:250. Confocal images of sagittal views of embryos were taken with a Zeiss LSM 510 META system and Z-series reconstructions were processed with the Zeiss LSM image acquisition program as previously described [23]. Statistical significance was assessed using the Bootstrap-test.

#### Additional files

**Additional file 1: Figure S1.** Alignment of STIM1 amino acid sequences of *Xenopus laevis*, *Xenopus tropicalis* and human. Identical amino acid residues are highlighted in dark. Dashes indicate gaps inserted for maximal alignment score. The red box indicates the amino acid (D65, within the EF hand motif) that was mutated in the dominant negative form of XSTIM1.

**Additional file 2: Figure S2.** Association of XSTIM1 with TRPC1. Shown are sample westernblots for co-immunoprecipitation of human TRPC1 (myc-hTRPC1-WT) and wild-type (YFP-XSTIM1-WT) or constitutively active STIM1 (YFP-XSTIM1-CA) expressed in *Xenopus* embryonic neural tissues.

**Additional file 3: Movie 1.** Filopodial  $\text{Ca}^{2+}$  entries are generated by SOCE. A pseudocolored Lck-GCaMP3 fluorescent  $\text{Ca}^{2+}$  images of *Xenopus* neuronal growth cones were captured at 200 milliseconds intervals over 7 min period of the store-depletion and re-addition of extracellular  $\text{Ca}^{2+}$  as shown in Figure 4A.

**Additional file 4: Movie 2.** SOCE-induced filopodial  $\text{Ca}^{2+}$  entries are abolished by inhibition of XSTIM1 with XSTIM1-DN overexpression. A pseudocolored Lck-GCaMP3 fluorescent  $\text{Ca}^{2+}$  images of *Xenopus* neuronal growth cones expressing XSTIM1-DN were captured at 200 milliseconds intervals over 7 min period of the store-depletion and re-addition of extracellular  $\text{Ca}^{2+}$ .

**Additional file 5: Movie 3.** SOCE-induced filopodial  $\text{Ca}^{2+}$  entries are attenuated by inhibition of XTRPC1 with XTRPC1-MO overexpression. A pseudocolored Lck-GCaMP3 fluorescent  $\text{Ca}^{2+}$  images of *Xenopus* neuronal growth cones expressing XTRPC1-MO were captured at 200 milliseconds intervals over 7 min period of the store-depletion and re-addition of extracellular  $\text{Ca}^{2+}$ .

**Additional file 6: Movie 4.** Oscillatory spontaneous filopodial  $\text{Ca}^{2+}$  entries. A pseudocolored Lck-GCaMP3 fluorescent  $\text{Ca}^{2+}$  images of *Xenopus* neuronal growth cones were captured at 200 milliseconds intervals over 7 min period in Modified Ringer solutions (1 mM extracellular  $\text{Ca}^{2+}$ ) as shown in Figure 5A.

**Additional file 7: Movie 5.** Spontaneous filopodial  $\text{Ca}^{2+}$  entries are abolished by inhibition of XSTIM1 with XSTIM1-DN overexpression. A pseudocolored Lck-GCaMP3 fluorescent  $\text{Ca}^{2+}$  images of *Xenopus* neuronal growth cones expressing XSTIM1-DN were captured at 200 milliseconds intervals over 7 min period in Modified Ringer solutions.

**Additional file 8: Movie 6.** Spontaneous filopodial  $\text{Ca}^{2+}$  entries are abolished by inhibition of XTRPC1 with XTRPC1-MO overexpression. A pseudocolored Lck-GCaMP3 fluorescent  $\text{Ca}^{2+}$  images of *Xenopus* neuronal growth cones expressing XTRPC1-MO were captured at 200 milliseconds intervals over 7 min period in Modified Ringer solutions.

**Additional file 9: Movie 7.** Netrin-1-potentiated filopodial  $\text{Ca}^{2+}$  entries. A pseudocolored Lck-GCaMP3 fluorescent  $\text{Ca}^{2+}$  images of *Xenopus* neuronal growth cone were captured at 200 milliseconds intervals in Modified Ringer solution (1 mM extracellular  $\text{Ca}^{2+}$ ) with Sp-cAMP (25  $\mu\text{M}$ ) before and after bath application of netrin-1 (10 ng/ml) as shown in Figure 4D.

**Additional file 10: Movie 8.** Dynamic translocation of STIM1 into neuronal filopodia in response to store-depletion. Time-lapse fluorescent images of *Xenopus* neuronal growth cone expressing YFP-XSTIM1 before (1 mM  $\text{Ca}^{2+}$ ) and after store  $\text{Ca}^{2+}$  depletion (0 mM  $\text{Ca}^{2+}$ /CPA). Images were captured at 2 seconds intervals.

#### Competing interests

The authors declare that they have no competing interests.

#### Authors' contributions

SS designed and performed all the experiments, and wrote the manuscript. JQZ oversaw the project, designed some of the experiments, and revised the manuscript with SS. GLM provided guidance to the project and contributed to the writing of the manuscript. All authors read and approved the final manuscript.

#### Acknowledgements

We thank P.F. Worley for help and discussion. This work was supported in part by grants from National Institutes of Health to JQZ (GM083889 and GM084363) and to GLM. (NS048271 and HD069184).

#### Author details

<sup>1</sup>Departments of Cell Biology and Neurology, Emory University School of Medicine, Atlanta, GA 30078, USA. <sup>2</sup>Center for Neurodegenerative Diseases, Emory University School of Medicine, Atlanta, GA 30322, USA. <sup>3</sup>Institute for Cell Engineering, Johns Hopkins University School of Medicine, Baltimore, MD 21205, USA. <sup>4</sup>Department of Neurology, Johns Hopkins University School of Medicine, Baltimore, MD 21205, USA. <sup>5</sup>The Solomon H. Snyder Department of Neuroscience, Johns Hopkins University School of Medicine, Baltimore, MD 21205, USA.

Received: 5 November 2013 Accepted: 23 November 2013

Published: 1 December 2013

#### References

- Zheng JQ, Poo MM: Calcium signaling in neuronal motility. *Annu Rev Cell Dev Biol* 2007, **23**:375–404.
- Cahalan MD: STIMulating store-operated  $\text{Ca}^{2+}$  entry. *Nat Cell Biol* 2009, **11**:669–677.
- Lewis RS: Store-operated calcium channels: new perspectives on mechanism and function. *Cold Spring Harb Perspect Biol* 2011, **3**(12). doi: 10.1101/cshperspecta.a003970.
- Kachoei BA, Knox RJ, Uthuz D, Levy S, Kaczmarek LK, Magoski NS: A store-operated  $\text{Ca}^{2+}$  influx pathway in the bag cell neurons of *Aplysia*. *J Neurophysiol* 2006, **96**:2688–2698.
- Li D, Herculat K, Oheim M, Ropert N: FM dyes enter via a store-operated calcium channel and modify calcium signaling of cultured astrocytes. *Proc Natl Acad Sci U S A* 2009, **106**:21960–21965.
- Gemes G, Bangaru ML, Wu HE, Tang Q, Weihrauch D, Koopmeiners AS, Cruikshank JM, Kwok WM, Hogan QH: Store-operated  $\text{Ca}^{2+}$  entry in sensory neurons: functional role and the effect of painful nerve injury. *J Neurosci* 2011, **31**:3536–3549.
- Venkiteswaran G, Hasan G: Intracellular  $\text{Ca}^{2+}$  signaling and store-operated  $\text{Ca}^{2+}$  entry are required in *Drosophila* neurons for flight. *Proc Natl Acad Sci U S A* 2009, **106**:10326–10331.
- Tang F, Kalil K: Netrin-1 induces axon branching in developing cortical neurons by frequency-dependent calcium signaling pathways. *J Neurosci* 2005, **25**:6702–6715.
- Baba A, Yasui T, Fujisawa S, Yamada RX, Yamada MK, Nishiyama N, Matsuki N, Ikegaya Y: Activity-evoked capacitative  $\text{Ca}^{2+}$  entry: implications in synaptic plasticity. *J Neurosci* 2003, **23**:7737–7741.
- Steinbeck JA, Henke N, Opatz J, Gruszczynska-Biegala J, Schneider L, Theiss S, Hamacher N, Steinfarz B, Golz S, Brustle O, et al: Store-operated calcium entry modulates neuronal network activity in a model of chronic epilepsy. *Exp Neurol* 2011, **232**:185–194.
- Geraldo S, Gordon-Weeks PR: Cytoskeletal dynamics in growth-cone steering. *J Cell Sci* 2009, **122**:3595–3604.
- Zheng JQ, Wan JJ, Poo MM: Essential role of filopodia in chemotropic turning of nerve growth cone induced by a glutamate gradient. *J Neurosci* 1996, **16**:1140–1149.
- Davenport RW, Dou P, Rehder V, Kater SB: A sensory role for neuronal growth cone filopodia. *Nature* 1993, **361**:721–724.
- Gomez TM, Robles E, Poo M, Spitzer NC: Filopodial calcium transients promote substrate-dependent growth cone turning. *Science* 2001, **291**:1983–1987.
- Nicol X, Hong KP, Spitzer NC: Spatial and temporal second messenger codes for growth cone turning. *Proc Natl Acad Sci U S A* 2011, **108**:13776–13781.
- Huang GN, Zeng W, Kim JY, Yuan JP, Han L, Muallem S, Worley PF: STIM1 carboxyl-terminus activates native SOC, I(crac) and TRPC1 channels. *Nat Cell Biol* 2006, **8**:1003–1010.
- Liu X, Cheng KT, Bandyopadhyay BC, Pani B, Dietrich A, Paria BC, Swaim WD, Beech D, Yildirim E, Singh BB, et al: Attenuation of store-operated  $\text{Ca}^{2+}$  current impairs salivary gland fluid secretion in TRPC1(-/-) mice. *Proc Natl Acad Sci U S A* 2007, **104**:17542–17547.
- Tojima T, Hines JH, Henley JR, Kamiguchi H: Second messengers and membrane trafficking direct and organize growth cone steering. *Nature reviews Neuroscience* 2011, **12**:191–203.
- Hong K, Nishiyama M, Henley J, Tessier-Lavigne M, Poo M: Calcium signalling in the guidance of nerve growth by netrin-1. *Nature* 2000, **403**:93–98.
- Shim S, Goh EL, Ge S, Sailor K, Yuan JP, Roderick HL, Bootman MD, Worley PF, Song H, Ming GL: XTRPC1-dependent chemotropic guidance of neuronal growth cones. *Nat Neurosci* 2005, **8**:730–735.
- Wang GX, Poo MM: Requirement of TRPC channels in netrin-1-induced chemotropic turning of nerve growth cones. *Nature* 2005, **434**:898–904.
- Tojima T: Intracellular signaling and membrane trafficking control bidirectional growth cone guidance. *Neurosci Res* 2012, **73**:269–274.
- Shim S, Yuan JP, Kim JY, Zeng W, Huang G, Milshteyn A, Kern D, Muallem S, Ming GL, Worley PF: Peptidyl-prolyl isomerase FKBP52 controls chemotropic guidance of neuronal growth cones via regulation of TRPC1 channel opening. *Neuron* 2009, **64**:471–483.
- Hogan PG, Lewis RS, Rao A: Molecular basis of calcium signaling in lymphocytes: STIM and ORAL. *Annu Rev Immunol* 2010, **28**:491–533.
- Shigetomi E, Kracun S, Khakh BS: Monitoring astrocyte calcium microdomains with improved membrane targeted GCaMP reporters. *Neuron Glia Biol* 2010, **6**:183–191.
- Kerstein PC, Jacques-Fricke BT, Rengifo J, Mogen BJ, Williams JC, Gottlieb PA, Sachs F, Gomez TM: Mechanosensitive TRPC1 channels promote calpain proteolysis of talin to regulate spinal axon outgrowth. *J Neurosci* 2013, **33**:273–285.
- Soboloff J, Rothberg BS, Madesh M, Gill DL: STIM proteins: dynamic calcium signal transducers. *Nature reviews Molecular cell biology* 2012, **13**:549–565.
- Song H, Ming G, He Z, Lehmann M, McKerracher L, Tessier-Lavigne M, Poo M: Conversion of neuronal growth cone responses from repulsion to attraction by cyclic nucleotides. *Science* 1998, **281**:1515–1518.
- Ming GL, Song HJ, Berninger B, Holt CE, Tessier-Lavigne M, Poo MM: cAMP-dependent growth cone guidance by netrin-1. *Neuron* 1997, **19**:1225–1235.
- Serafini T, Colamarino SA, Leonardo ED, Wang H, Beddington R, Skarnes WC, Tessier-Lavigne M: Netrin-1 is required for commissural axon guidance in the developing vertebrate nervous system. *Cell* 1996, **87**:1001–1014.
- Kennedy TE, Serafini T, de la Torre JR, Tessier-Lavigne M: Netrins are diffusible chemotropic factors for commissural axons in the embryonic spinal cord. *Cell* 1994, **78**:425–435.



32. Mitchell CB, Gasperini RJ, Small DH, Foa L: **STIM1 is necessary for store-operated calcium entry in turning growth cones.** *J Neurochem* 2012, **122**:1155–1166.
33. Li Y, Jia YC, Cui K, Li N, Zheng ZY, Wang YZ, Yuan XB: **Essential role of TRPC channels in the guidance of nerve growth cones by brain-derived neurotrophic factor.** *Nature* 2005, **434**:894–898.
34. Ming G, Song H, Berninger B, Inagaki N, Tessier-Lavigne M, Poo M: **Phospholipase C-gamma and phosphoinositide 3-kinase mediate cytoplasmic signaling in nerve growth cone guidance.** *Neuron* 1999, **23**:139–148.
35. Takei K, Shin RM, Inoue T, Kato K, Mikoshiba K: **Regulation of nerve growth mediated by inositol 1,4,5-trisphosphate receptors in growth cones.** *Science* 1998, **282**:1705–1708.
36. Akiyama H, Matsu-ura T, Mikoshiba K, Kamiguchi H: **Control of neuronal growth cone navigation by asymmetric inositol 1,4,5-trisphosphate signals.** *Sci Signal* 2009, **2**:ra34.
37. Xie Y, Hong Y, Ma XY, Ren XR, Ackerman S, Mei L, Xiong WC: **DCC-dependent phospholipase C signaling in netrin-1-induced neurite elongation.** *J Biol Chem* 2006, **281**:2605–2611.
38. Xie Y, Ding YQ, Hong Y, Feng Z, Navarre S, Xi CX, Zhu XJ, Wang CL, Ackerman SL, Kozlowski D, et al: **Phosphatidylinositol transfer protein-alpha in netrin-1-induced PLC signalling and neurite outgrowth.** *Nat Cell Biol* 2005, **7**:1124–1132.
39. Yuan JP, Kim MS, Zeng W, Shin DM, Huang G, Worley PF, Muallem S: **TRPC channels as STIM1-regulated SOCs.** *Channels (Austin)* 2009, **3**:221–225.
40. Yuan JP, Zeng W, Huang GN, Worley PF, Muallem S: **STIM1 heteromultimerizes TRPC channels to determine their function as store-operated channels.** *Nat Cell Biol* 2007, **9**:636–645.
41. Kim MS, Zeng W, Yuan JP, Shin DM, Worley PF, Muallem S: **Native Store-operated Ca<sup>2+</sup> Influx Requires the Channel Function of Orai1 and TRPC1.** *J Biol Chem* 2009, **284**:9733–9741.
42. Grigoriev I, Gouveia SM, van der Vaart B, Demmers J, Smyth JT, Honnappa S, Splinter D, Steinmetz MO, Putney JW Jr, Hoogenraad CC, Akhmanova A: **STIM1 is a MT-plus-end-tracking protein involved in remodeling of the ER.** *Curr Biol* 2008, **18**:177–182.
43. Lefkimiatis K, Srikanthan M, Maiellaro I, Moyer MP, Curci S, Hofer AM: **Store-operated cyclic AMP signalling mediated by STIM1.** *Nat Cell Biol* 2009, **11**:433–442.
44. Cheng KT, Liu X, Ong HL, Swaim W, Ambudkar IS: **Local Ca(2) + entry via Orai1 regulates plasma membrane recruitment of TRPC1 and controls cytosolic Ca(2) + signals required for specific cell functions.** *PLoS Biol* 2011, **9**:e1001025.
45. Ong HL, Cheng KT, Liu X, Bandyopadhyay BC, Paria BC, Soboloff J, Pani B, Gwack Y, Srikanth S, Singh BB, et al: **Dynamic assembly of TRPC1-STIM1-Orai1 ternary complex is involved in store-operated calcium influx. Evidence for similarities in store-operated and calcium release-activated calcium channel components.** *J Biol Chem* 2007, **282**:9105–9116.
46. Shigetomi E, Tong X, Kwan KY, Corey DP, Khakh BS: **TRPA1 channels regulate astrocyte resting calcium and inhibitory synapse efficacy through GAT-3.** *Nat Neurosci* 2012, **15**:70–80.
47. Shekarabi M, Kennedy TE: **The netrin-1 receptor DCC promotes filopodia formation and cell spreading by activating Cdc42 and Rac1.** *Mol Cell Neurosci* 2002, **19**:1–17.
48. Robles E, Woo S, Gomez TM: **Src-dependent tyrosine phosphorylation at the tips of growth cone filopodia promotes extension.** *J Neurosci* 2005, **25**:7669–7681.
49. Han J, Han L, Tiwari P, Wen Z, Zheng JQ: **Spatial targeting of type II protein kinase A to filopodia mediates the regulation of growth cone guidance by cAMP.** *J Cell Biochem Suppl* 2007, **176**:101–111.
50. Mattila PK, Lappalainen P: **Filopodia: molecular architecture and cellular functions.** *Nature reviews Molecular cell biology* 2008, **9**:446–454.
51. Dent EW, Gupton SL, Gertler FB: **The growth cone cytoskeleton in axon outgrowth and guidance.** *Cold Spring Harb Perspect Biol* 2011, **3**(3). doi: 10.1101/cshperspect.a001800.
52. Gomez TM, Snow DM, Letourneau PC: **Characterization of spontaneous calcium transients in nerve growth cones and their effect on growth cone migration.** *Neuron* 1995, **14**:1233–1246.
53. Wedel B, Boyles RR, Putney JW Jr, Bird GS: **Role of the store-operated calcium entry proteins Stim1 and Orai1 in muscarinic cholinergic receptor-stimulated calcium oscillations in human embryonic kidney cells.** *J Physiol* 2007, **579**:679–689.
54. Bird GS, Hwang SY, Smyth JT, Fukushima M, Boyles RR, Putney JW Jr: **1STIM1 is a calcium sensor specialized for digital signaling.** *Curr Biol* 2009, **19**:1724–1729.
55. Di Capite J, Ng SW, Parekh AB: **Decoding of cytoplasmic Ca(2+) oscillations through the spatial signature drives gene expression.** *Curr Biol* 2009, **19**:853–858.
56. Ming GL, Wong ST, Henley J, Yuan XB, Song HJ, Spitzer NC, Poo MM: **Adaptation in the chemotactic guidance of nerve growth cones.** *Nature* 2002, **417**:411–418.
57. Harland RM: **In situ hybridization: an improved whole-mount method for Xenopus embryos.** *Methods Cell Biol* 1991, **36**:685–695.
58. Lohof AM, Quillan M, Dan Y, Poo MM: **Asymmetric modulation of cytosolic cAMP activity induces growth cone turning.** *J Neurosci* 1992, **12**:1253–1261.
59. Zheng JQ, Felder M, Connor JA, Poo MM: **Turning of nerve growth cones induced by neurotransmitters.** *Nature* 1994, **368**:140–144.
60. Rivas RJ, Burmeister DW, Goldberg DJ: **Rapid effects of laminin on the growth cone.** *Neuron* 1992, **8**:107–115.
61. Hopker VH, Shewan D, Tessier-Lavigne M, Poo M, Holt C: **Growth-cone attraction to netrin-1 is converted to repulsion by laminin-1.** *Nature* 1999, **401**:69–73.
62. Gomez TM, Spitzer NC: **In vivo regulation of axon extension and pathfinding by growth-cone calcium transients.** *Nature* 1999, **397**:350–355.
63. Pheps PE, Alijani A, Tran TS: **Ventrally located commissural neurons express the GABAergic phenotype in developing rat spinal cord.** *J Comp Neurol* 1999, **409**:285–298.

doi:10.1186/1756-6606-6-51

**Cite this article as:** Shim et al.: A critical role for STIM1 in filopodial calcium entry and axon guidance. *Molecular Brain* 2013 **6**:51.

**Submit your next manuscript to BioMed Central and take full advantage of:**

- Convenient online submission
- Thorough peer review
- No space constraints or color figure charges
- Immediate publication on acceptance
- Inclusion in PubMed, CAS, Scopus and Google Scholar
- Research which is freely available for redistribution

Submit your manuscript at  
www.biomedcentral.com/submit

